ARTICLE TYPE

Traffic emission factors of ultrafine particles

Effects from ambient air

Sara Janhäll,*[a,c] Peter Molnar[b] and Mattias Hallquist[c]

Received (in XXX, XXX) Xth XXXXXXXXX 20XX, Accepted Xth XXXXXXXXX 20XX

DOI:

Ultrafine particles have a significant detrimental effect on both human health and climate. In order to abate this problem, it is necessary to identify the sources of ultrafine particles. A parameterisation method is presented for estimating the levels of traffic-emitted ultrafine particles in terms of variables describing the ambient conditions. The method is versatile and could easily be applied to similar data sets in other environments. The data used were collected during a four-week period in February 2005, in Gothenburg, as part of the Göte-2005 campaign. The specific variables tested were temperature (T), relative humidity (RH), carbon monoxide concentration (CO), and the concentration of particles up to 10 µm in diameter (PM_{10}); all indicators of importance for aerosol processes such as coagulation and gas-particle partitioning. These variables were selected because of their direct effect on aerosol processes (T and RH) or as proxies for aerosol surface-area (CO and PM_{10}), and because of their availability in local monitoring programmes, increasing the usability of the parameterization. Emission factors are presented for 10–100-nm particles (ultrafine particles; EF_{ufp}), for 10–40-nm particles ($EF_{10–40}$), and for 40–100-nm particles ($EF_{40–100}$). For $EF_{40–100}$ no effect of ambient conditions was found. The emission factor equations are calculated based on an emission factor for NO_x of 1 g km^{-1}, thus the particle emission factors are easily expressed in units of particles per gram of NO_x emitted. Alternative equations for the EFs in terms of temperature and PM_{10} concentration are also presented.

Introduction

Traffic is a major contributor to particulate air pollution in urban areas, producing particles of all sizes from coarse (2.5–10 µm in diameter), emitted from resuspension and wear, to ultrafine (less than 100 nm in diameter), freshly emitted from the tailpipe. [1] The majority of health studies use PM_{10} or $PM_{2.5}$, i.e. larger particle sizes (up to 10 or 2.5 µm in diameter, respectively), as the particle exposure estimate, owing to the availability of long time-series of monitoring data. The available data on ultrafine particles are still too limited to be used in epidemiological studies.

Traffic-related air pollution has long been known to affect the health of the general population. Grahame and Schlesinger[2] concluded that epidemiological studies consistently find associations between exposure to particulate emissions from motor vehicles and cardiopulmonary and cardiovascular endpoints. They also referred to mechanistic studies that support a pathophysiological basis for how diesel and/or vehicular emissions could cause such outcomes.

Several studies have shown that fine particles have adverse effects on health, both in the short term[3-5] and in the long term.[6, 7] Evidence of adverse health effects being caused by ultrafine particles has also been presented in the last decade,[8, 9] with the conclusion that ultrafine particles seem to be at least as potent as fine particles for several morbidity and mortality health outcomes. In particular, the concern over adverse human health effects of ultrafine particles has highlighted the need for accurate descriptions of particle exposure[10] including the best possible particle emission factors from vehicle traffic.

Ultrafine particles emitted from traffic are principally of two types: soot-containing particles, in the 60–100 nm range, and nucleated droplet particles, in which a kernel of sulphate acts as a deposition surface for condensed exhaust gases, creating particles less than 20 nm in diameter.[11, 12] The soot particles are produced before exiting the tail-pipe, but may grow in size owing to condensation of vapours (e.g. sulphuric acid and low-volatile organics) onto their surface. The nucleated droplet particles are produced in the dilution process when hot exhaust is mixed with ambient air with concurrent cooling, and their final number and sizes depend on the dilution process and properties of the ambient air.[13, 14] This initial dilution stage is usually termed tailpipe-to-road. It can persist for 1–3 seconds after tailpipe emission and may dilute the exhaust by a factor of more than 1000.[15] The properties of the ambient air, such as temperature and available condensatino sink, will determine the number and the size-distribution of the emitted particles. In addition to this initial dilution, a second, much slower process takes place, termed road-to-ambient, which takes up to 10 minutes and results in dilution by a factor of about 10.[15] Both these steps include transformation processes—condensation, evaporation, deposition, nucleation, and dilution, in varying amounts dependent on the ambient air. The compounds evaporated during the dilution steps are likely to

contribute to atmospheric aerosol formation after being oxidised.[16, 17] For an urban plume, the ratio of total to primary aerosol can quickly grow to values of 2 to 5.[18]

Today, there is extensive information on how vehicle characteristics, such as fuel type and engine load, and fleet characteristics, such as proportion of heavy-duty vehicles, affect the level of emission of ultrafine particles.[13, 19] However, particle number, and in this context also particle mass, are not conserved during the dilution stages, the point at which the emission is characterised thus affects the derived emission factor significantly.[13, 20] The determination of derived emission factors should at least take account of the tailpipe-to-road dilution stage, while the second stage may be treated using aerosol dynamic modelling.[21, 22] In order to be of direct use for air-quality modelling, the applied emission factor should be linked to the spatial scale of concern, for example, street canyon, urban background, or rural environment.[20] In addition to the distance from the traffic emission source, there is an obvious variation in composition and intensity of the traffic fleet for different environments. Consequently, there is a need to describe emissions at numerous locations and during different conditions. Application of the emission-factor method described by Janhäll and Hallquist[23] allows the derivation of size-distributed traffic emission factors for ultrafine particle–number from single-point measurements. Owing to its rather straightforward approach, the amount of measurement data needed to derive emission factors is significantly reduced, enabling a [23, 24]significant expansion of the emission factor database. As the traffic relation is derived from gas concentrations and not directly from traffic intensity, it is possible to take measurements at larger distances from traffic, and the time evolution of the urban plume is easily studied. The method was also designed to provide emission factors for non-temporal data sets and is thus extremely valuable for the study of ambient effects on particle emissions.

The present study extends these methods to investigate the influence of ambient dilution conditions on particle-number emission factors. The focus of the study was on the variables expected to have a significant effect on the emission of ultrafine particles: ambient temperature (T), relative humidity (RH), and available condensation sink. For available condensation sink the use of carbon monoxide (CO) and particulate matter (PM_{10}) concentrations as proxies was evaluated, since data on these variables are frequently available at typical monitoring stations.

Methods

Over a four-week period, 2 February to 2 March 2005, an international measurement campaign, Göte-2005, was conducted in Gothenburg, Sweden (57° N 11° E), an urban region of 600,000 inhabitants. The measurements were conducted on a rooftop, 30 m above ground level, in the city centre (the Femman monitoring site), as described elsewhere.[23, 24] The amount of heavy duty traffic in this area is 10%. As part of this campaign, the particle-number size-distribution, for particles 10–100 nm in diameter, was obtained with a Scanning Mobility Particle Sizer (SMPS) from TSI (DMA 3081, CPC 3022) every 5 minutes. Other variables measured at the same site were gas concentrations—NO and NO_2 (Chemiluminiscence, Ecophysics Tecan 700 AL), CO (NDIR, Maihak UNOR 610), and O_3 (Monitor Labs 9811)—, PM_{10} concentration (TEOM, Rupprecht & Patashnick 1400), and meteorological data—temperature and relative humidity (Campbell Rotometric, MP101), and wind speed and wind direction (Gill Ultrasonic). The total dataset used for analysis comprised 7099 records at five-minute intervals. Arithmetic means of selected variables are given in Table 1.

Generally, the weather was normal for this site in February: the temperature was mostly below zero, it was windy and cloudy, and 20% of the measurements were taken during precipitation (of rain/snow). As has been noted in previous studies, the measurement site is frequently exposed to air masses containing local traffic exhausts, as shown, for example, by the correlation between the concentrations of nitrogen oxides, carbon monoxide, and particles in the size range 20–100 nm, and by a weak negative correlation between the levels of those pollutants and wind speed.[25-27] In addition, concurrent measurements during the Göte-2005 campaign showed a low impact from wood combustion that otherwise might be a significant combustion source of particles.[28] The general air pollution situation at this site during the campaign has been described elsewhere.[24, 29]

Table 1. Arithmetic mean ± standard deviation of meteorological and air quality parameters over the full campaign, i.e. 7099 data points, with units.

Variable	Unit	Mean	Standard deviation	Min	Max
Temperature	°C	−0.8	3.3	−9.7	5.6
Wind Speed	$m\ s^{-1}$	4.4	2.4	0.2	13.4
Precipitation	$mm\ hr^{-1}$	0.3	0.9	0	6.6
RH	%	82	12	31	99.6
Pressure	hPa	1016	11	974	1033
CO	$mg\ m^{-3}$	0.128	0.145	0	0.378
NO	$\mu g\ m^{-3}$	14	39	0	654
NO_2	$\mu g\ m^{-3}$	28	20	0	265
NO_x	$\mu g\ m^{-3}$	50	76	2	1255
Ozone	$\mu g\ m^{-3}$	54	25	3	132
PM_{10}	$\mu g\ m^{-3}$	21	21	0	300
PN	$10^4\ cm^{-3}$	1.38	1.15	0.1	9.6

Particle-number emission factor

The particle-number emission factor, EF_{PN}, was derived according to the method described in Janhäll and Hallquist,[23] and for convenience is also briefly described below. The calculation is based on a dataset of size-distributed particle-number concentration and NO and NO_2 concentrations measured every 5 minutes in a traffic-affected area. The NO and NO_2 concentrations are used to classify measurements according to whether the site is exposed to air containing high levels of traffic emission or to background air.

The high-traffic-exposure data (corresponding to fresh traffic exhaust) are defined as those records with an NO to NO_2 ratio in the upper quintile of the dataset as a whole and the high-traffic particle-number and NOx concentrations, $PN_{high\text{-}traffic}$ and $NOx_{high\text{-}traffic}$, are defined as the corresponding averages over this subset. The background data are defined as those records with a NOx concentration in the lower quintile of the dataset as a whole and the background particle-number and NOx concentrations, PN_{bkg} and NOx_{bkg}, are defined as the corresponding averages over this subset. As described in detail by Janhäll and Hallquist,[23] given these quantities and the emission factor for NOx, EF_{NOx},

the absolute emission factor of size-distributed ultrafine particles is given by Eq. 1.

$$EF_{PN} = \frac{PN_{hightraffic} - PN_{bkg}}{NOx_{hightraffic} - NOx_{bkg}} * EF_{NOx} \quad (1)$$

EF_{NOx} was taken to be 1 g km^{-1}, based on Swedish conditions in 2005 and 10% heavy duty vehicles in the area. The emission factor can also be used directly as the ratio between particle and NOx emissions.

Measurement plan – data treatment

Size-distributed emission factors were derived by calculating separate emission factors for each of the channels of the SMPS system (64 channels/decade distributed logarithmically over, in this case, 10–100 nm). For the regression modelling, emissions factors were also calculated according to the total number of emitted particles in three size classes: ultrafine particles (10–100 nm), nucleation droplet–dominated fraction (10–40 nm), and soot-dominated fraction (40–100 nm). This division into two size-bins was used to estimate separate regressions for each of these two dynamically different modes.

For each of the four variables T, RH, CO, and PM_{10}, the full dataset was sorted and divided into quintiles; resulting in five equally sized subsets for each variable. For each of the subsets, the particle-number emission factor was calculated for all channels in the size distribution as well as for the three size classes, 10–100 nm, 10–40 nm, and 40–100 nm. The calculated emission factors are referred to as EF_{ufp} for particles between 10 and 100 nm, $EF_{10–40}$ for particles between 10 and 40 nm, and $EF_{40–100}$ for particles between 40 and 100 nm. The emission factors (EFs) for each specific subset were calculated as described above, using the NOx concentration and NO to NO_2 ratio to define the background and high-traffic conditions, respectively. To characterise each subset, the average of the respective variable was calculated using the data in the "high traffic" part of the subset, since the emissions would be affected by the ambient conditions at the time of emission.

From the five calculated EFs per studied variable a relation between the variable and the particle emissions was estimated by linear fitting. The statistical calculations were performed using the SAS System for Windows, version 9.2. The models were estimated with Proc Reg and the selection criteria used were the coefficient of determination, r^2; Mallow's Cp; and the mean standard error. Statistical significance refers to $p < 0.05$ in two-tailed tests.

Results

The correlation analysis of this highly time-resolved dataset mainly showed the high positive correlation between the levels of traffic-emitted compounds—carbon monoxide (CO) and nitrogen oxides (NO, NO_2, and NOx)—and the level of ultrafine particles, as well as a negative correlation of these with the level of ozone (O_3). In this study, we focussed on a set of variables—T, RH, CO, and PM_{10}—that are either proxies for or directly physically related to the variables affecting the initial particle dynamics. However, as an initial example of how weather conditions affect ultrafine-particle concentrations and emission factors differently, the data were divided into measurements taken in precipitating and in non-precipitating conditions.

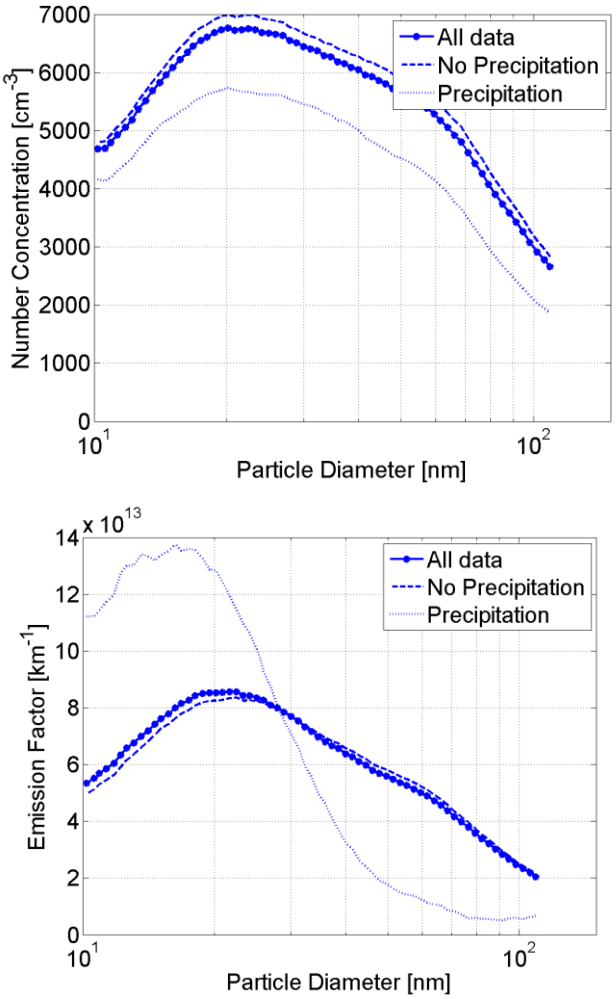

Fig. 1 Particle size distribution of (a) number concentration, and (b) emission factor, for the full data set and the two subsets without and with precipitation.

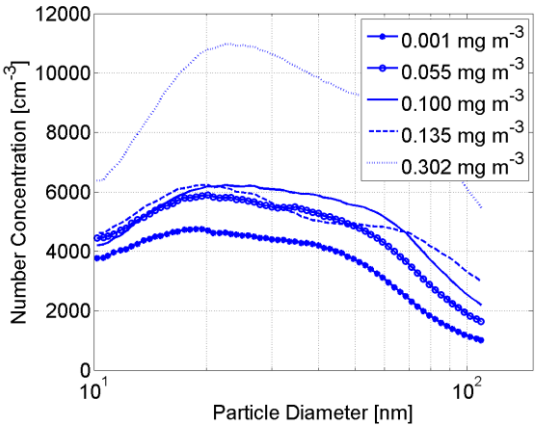

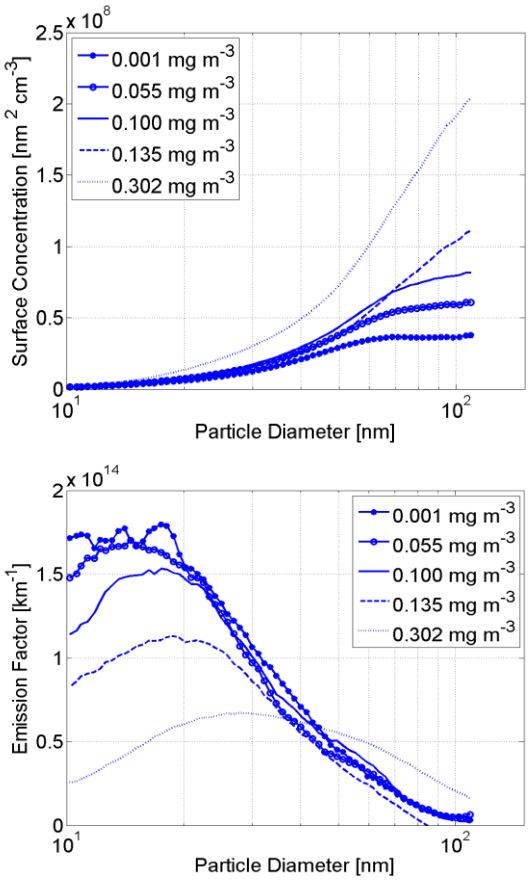

Fig. 2 Particle size distribution for the five subsets defined by CO-concentration quintiles of (a) number concentration, (b) surface area concentration, and (c) particle-number emission factor. The average CO concentration for each quintile is shown in the legend.

Figure 1a shows the averaged particle-number size-distributions for the full data set and for the two subsets, precipitation (1/5 of the overall data) and no precipitation (4/5 of the overall data). Here, the lower concentration of particle numbers in precipitating conditions is clearly visible. $EF_{10–40}$, the emission factor for particles in the lower size range of 10–40 nm, was almost doubled for the precipitation data set (Figure 1b). This is attributable to the fact that any precipitation will decrease the available surface area for deposition of potential nucleation species. Precipitation had a negative effect on the $EF_{40–100}$, for 40–100-nm particles, since precipitation will scavenge these during their transport from the tail-pipe of the vehicle to the rooftop measurement site. The precipitation was, for most of the time, in the form of heavy snowfall, which may be even more efficient in scavenging particles than typical rain.[30]

The example with precipitation is rather simple since there are two distinct conditions. For the variables selected for modelling—T, RH, PM_{10}, and CO—there are gradients in the conditions and the subset was, as described above, divided into five subsets for each variable. Using CO as an example, Figure 2 shows the average particle concentration for each of the five subsets defined by the CO-concentration quintiles in terms of (a) particle number, and (b) particle surface area. The average CO concentration for each of the subsets is given in the figures. Figure 2b clearly illustrates the relationship between surface-area concentration and CO concentration and validates the use of CO concentration as a proxy for condensation sink, even though only particles below 100 nm were measured. In analogy to the example of precipitation, Figure 2c shows the derived particle-number emission factors for the five CO-concentration subsets. The emissions clearly increase with decreasing CO concentration, mainly in the lower particle-size ranges. Similar results were obtained for the other variables and the corresponding data were used for the regression estimation presented below.

Parameterisation of emission factor

Emission factors were calculated for each of the 15 subsets defined by the quintiles of temperature, carbon monoxide concentration, and PM_{10} concentration. Each subset was characterised by the average of the corresponding variable (T, CO, or PM_{10}) over the high-traffic part of the subset, this being the condition for the emission processes considered. Figure 3 shows $EF_{10–40}$ and $EF_{40–100}$ versus each of the variables—(a) temperature, (b) carbon monoxide concentration, and (c) PM_{10} concentration. All three variables affected $EF_{10–40}$ (solid line), while $EF_{40–100}$ (solid line with markers) did not exhibit the same sensitivity, as anticipated.

In order to derive a mathematical description of the relationship between the variables and the emission factors, several regression models were tested. Multiple linear regression was used to explain the variation in EF for ultrafine particles (10–100 nm), for the nucleation fraction (10–40 nm), and for the soot fraction (40–100 nm). The carbon monoxide concentration in mg m^{-3} (CO), the temperature in kelvins (T), the relative humidity as a percentage (RH), and the particle concentration in µg m^{-3} (PM_{10}) were included in the models, both individually and in combinations, i.e. using one to four explanatory variables.

Models including other orders of the base variables, e.g. T^2 and $CO^{1/2}$, were also tested in order to investigate any non-linear behaviour. A selection of the models is presented in Tables 2 and 3, showing for each model the variables included, the value of the F-statistic, its corresponding p-value, and the coefficient of determination, r^2, and for each variable in each model its parameter estimate, the value of the t-statistic for including the variable in the model, and its corresponding p-value. The criteria for a valid model were that the full model must pass the F-test, i.e. be significant, and that all components (i.e. intercept and variables) must contribute significantly to the model.

For ultrafine particles, the CO concentration on its own explains a most of the variation ($r^2 = 0.68$) in the emission factor, EF_{ufp}. The inclusion of both CO and T increases the variation explained to 0.80, giving the most favourable model (see Table 2): $EF_{ufp} = 1.81\times10^{15} - 1.71\times10^{14}\times CO - 5.88\times10^{12}\times T$, which can be rearranged to give Eq. 2 (in particles km^{-1}).

$$EF_{ufp} = 1.8\times10^{15}\times(1 - 0.095\times CO - 3.2\times10^{-3}\times T) \quad (2)$$

Table 2. Tested models for the regression of EF_{ufp}. First the four one-parameter models, followed by the higher-order parameter models for which all parameters significantly contributed to the explanation. Presented are the variable name, parameter estimate, *t*-value and *p*-value for the estimate, the *F*-value and *p*-value for the whole model, and r^2.

Variable	Parameter estimate	*t*	*p* > |*t*|	*F*	*p* > *F*	r^2
One-parameter models for EF_{ufp}						

Intercept	2.22×10^{14}	21.09	<.0001	30.12	0.0001	0.68
CO	-2.15×10^{14}	−5.49	0.0001			
Intercept	3.20×10^{15}	3.47	0.0041	10.80	0.0059	0.45
Temp	-1.11×10^{13}	−3.29	0.0059			
Intercept	1.86×10^{14}	9.25	<.0001	0.51	0.4865	0.04
PM_{10}	-4.58×10^{11}	−0.72	0.4865			
Intercept	4.36×10^{14}	3.01	0.0100	3.29	0.0928	0.20
RH	-3.38×10^{12}	−1.81	0.0928			
Two-parameter models for EF_{ufp}						
Intercept	1.81×10^{15}	2.73	0.0183	23.41	<.0001	0.80
Temp	-5.88×10^{12}	−2.39	0.0338			
CO	-1.71×10^{14}	−4.49	0.0007			
Intercept	4.05×10^{15}	5.07	0.0003	12.38	0.0012	0.67
Temp	-1.41×10^{13}	−4.83	0.0004			
PM_{10}	-1.18×10^{12}	−2.84	0.0148			
Intercept	7.38×10^{14}	4.84	0.0004	7.09	0.0093	0.54
PM_{10}	-1.71×10^{12}	−2.98	0.0114			
RH	-6.68×10^{12}	−3.63	0.0034			
Three-parameter models for EF_{ufp}						
Intercept	3.44×10^{15}	5.48	0.0002	18.13	0.0001	0.83
Temp	-1.07×10^{13}	−4.36	0.0011			
PM_{10}	-1.79×10^{12}	−4.91	0.0005			
RH	-4.18×10^{12}	−3.22	0.0082			

Most of the dynamics affecting EF_{ufp} are due to dynamics in the Aitken mode and thus the tested models for $EF_{10–40}$ gave similar results as for EF_{ufp} (see Table 3), but with a slightly higher degree of explanation ($r^2 = 0.88$). The chosen model is given in Eq. 3 (in particles km^{-1}).

$$EF_{10–40} = 2.1\times10^{15}\times(1 - 0.099\times CO - 3.4\times10^{-3}\times T) \quad (3)$$

The negative correlation between the emission factors and CO concentration is expected since CO is a tracer of air pollution and thus also for available condensation sink. The negative temperature dependence is due to faster condensation processes at lower temperatures.

As a comparison, the equations for the EFs related to temperature and PM_{10} concentration are also presented in Eqs. 4-5 in particles per km. Here, PM_{10} is used as a tracer of air pollution and, following the discussion for carbon monoxide above, the negative correlation with EF is anticipated.

$$EF_{ufp} = 4.0\times10^{15}\times(1 - 2.9\times10^{-4}\times PM_{10} - 3.5\times10^{-3}\times T) \quad (4)$$

$$EF_{10-40} = 4.7\times10^{15}\times(1 - 2.9\times10^{-4}\times PM_{10} - 3.6\times10^{-3}\times T) \quad (5)$$

For the emission factor for larger particles, $EF_{40–100}$, the degree of explanation was low for all tested models ($r^2 < 0.36$) and the F-tests did not show significance except for the model including only CO ($r^2 = 0.32$), see Table 3. The concentration of particles in the 40–100 nm range did not differ much between plume conditions and background air, resulting in the lower statistical significance. Since $EF_{40–100}$ does not vary much over the measured ranges of the tested variables (see Figure 3), a constant EF is suggested for this size interval, see Eq. 6.

$$EF_{40–100} = 3.9\times10^{13} \pm 1.1\times10^{13} \text{ particles km}^{-1} \quad (6)$$

Table 3. Tested models for the regressions of $EF_{10–40}$ and $EF_{40–100}$. For $EF_{10–40}$ the four one-parameter models are presented first, followed by the higher-order parameter models for which all parameters significantly contributed to the explanation. For $EF_{40–100}$ only one model is presented. Presented are the variable name, parameter estimate, *t*-value and *p*-value for the estimate, the *F*-value and *p*-value for the whole model, and r^2.

Variable	Parameter estimate	*t*	$p > \|t\|$	*F*	$p > F$	r^2
One-parameter models for $EF_{10–40}$						
Intercept	1.92×10^{14}	18.66	<.0001	44.78	<.0001	0.78
CO	-2.57×10^{14}	−6.69	<.0001			
Intercept	3.73×10^{15}	3.73	0.0025	12.93	0.0033	0.50
Temp	-1.32×10^{13}	−3.60	0.0033			
Intercept	1.48×10^{14}	6.48	<.0001	0.47	0.505	0.03
PM_{10}	-4.97×10^{11}	−0.69	0.5050			
Intercept	4.45×10^{14}	2.75	0.0164	3.71	0.0763	0.22
RH	-4.01×10^{12}	−1.93	0.0763			
Two-parameter models for $EF_{10–40}$						
Intercept	2.07×10^{15}	3.60	0.0037	44.32	<.0001	0.88
Temp	-6.94×10^{12}	−3.26	0.0068			
CO	-2.05×10^{14}	−6.20	<.0001			
Intercept	4.70×10^{15}	5.63	0.0001	15.62	0.0005	0.72
Temp	-1.67×10^{13}	−5.45	0.0001			
PM_{10}	-1.35×10^{12}	−3.11	0.0090			
Intercept	7.92×10^{14}	4.72	0.0005	7.92	0.0064	0.57
PM_{10}	-1.96×10^{12}	−3.11	0.0090			
RH	-7.79×10^{12}	−3.86	0.0023			
Three-parameter models for $EF_{10–40}$						
Intercept	4.00×10^{15}	6.85	<.0001	28.73	<.0001	0.89
Temp	-1.26×10^{13}	−5.56	0.0002			
PM_{10}	-2.05×10^{12}	−6.06	<.0001			
RH	-4.82×10^{12}	−4.00	0.0021			
Model for EF_{40-100}						
Intercept	2.98×10^{13}	6.55	<.0001	6.06	0.0286	0.32
CO	4.16×10^{13}	2.46	0.0286			

Figure 4 shows a comparison between the values of EF_{ufp} and $EF_{10–40}$ obtained directly from the data (points) and the values calculated with Eqs. 2–5 using the average CO or PM_{10} concentrations and the average temperature, for each temperature subset. The emission factors calculated using the models reproduce the measured data well, although the number of data points is limited. The variation in the EFs that is not explained by a linear relation to temperature alone is better explained by including CO in the model (solid line) than by including PM_{10} in the model (broken line). Thus we recommend using the formulae in T and CO to estimate EF, if such data are available.

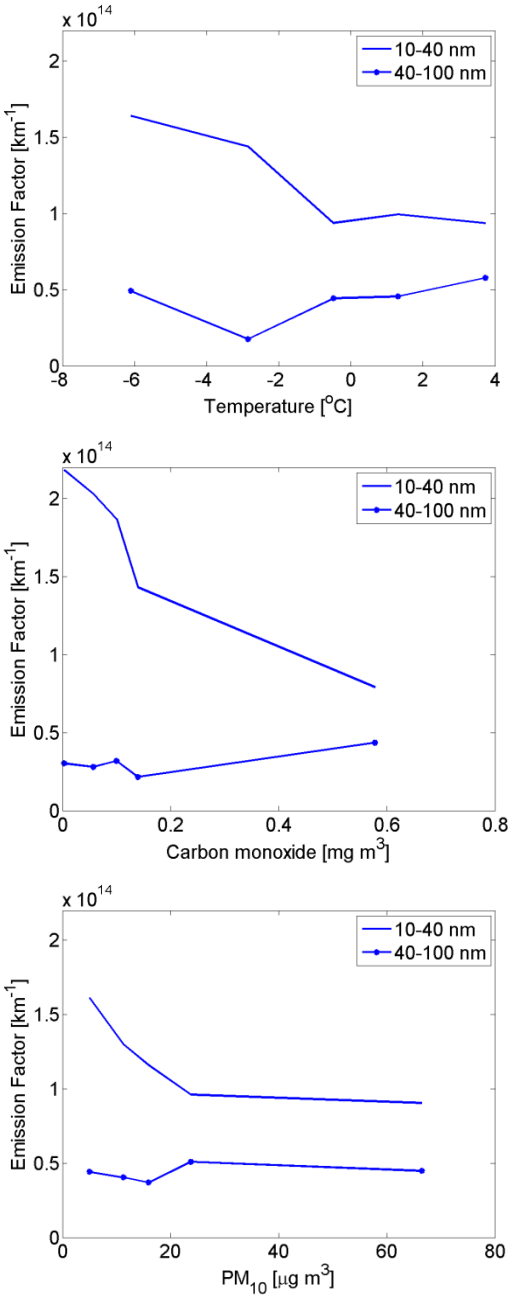

Fig. 3 $EF_{10–40}$ and $EF_{40–100}$ versus (a) temperature, (b) carbon monoxide concentration, and (c) PM_{10} concentration. The EFs were calculated for the corresponding quintile-defined subsets and plotted against the average of the corresponding variable over the high-traffic part of the subset.

The emission factor estimate for the smaller particle-size range, $EF_{10–40}$, was in closer agreement with the data than was the estimate for the full ultrafine particle-size range, EF_{ufp}, indicating that different parts of the ultrafine particle-size range behave differently. Figure 5 compares the EF_{ufp} obtained directly from the data (points) with the estimate of EF_{ufp} (solid line) and the sum of the estimates of $EF_{10–40}$ and $EF_{40–100}$ (broken line), using the formulae in T and CO recommended above. At lower temperatures there is no difference between the two ways to calculate the emission of 10–100-nm particles, while for temperatures above zero the estimate for the entire range, EF_{ufp}, is larger than the sum of the estimates for the two size bins, see Figure 5.

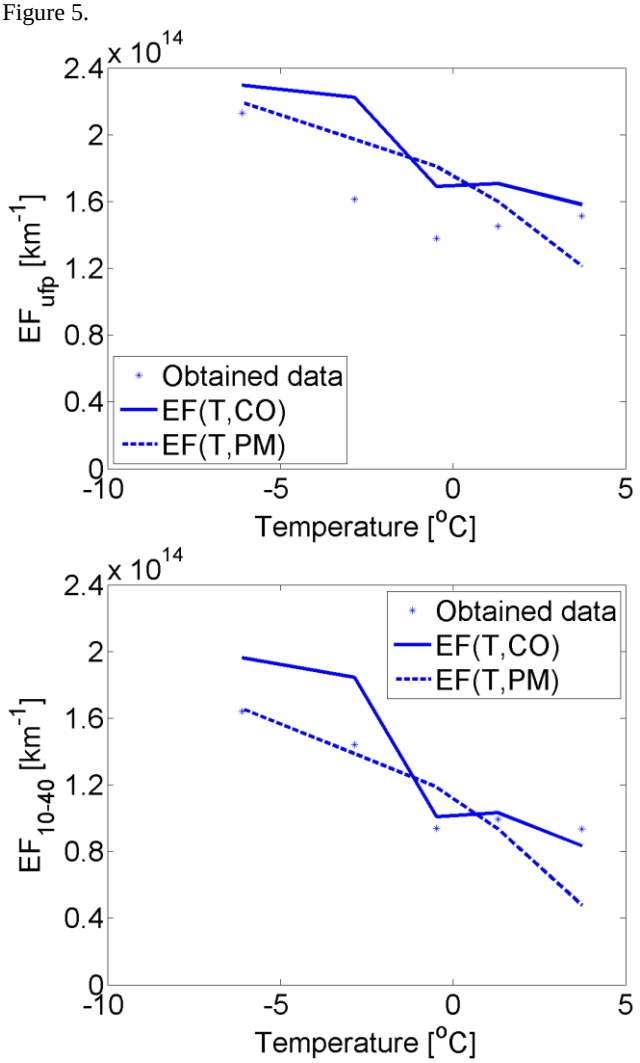

Fig. 4 (a) EF_{ufp} and (b) $EF_{10–40}$ versus temperature, obtained directly from the data (points), calculated from the regression on T and CO (solid line), and calculated from the regression on T and PM_{10} (broken line).

This shows that treating the different size modes separately leads to a slightly larger estimate of the temperature effect than when modelling the data as a whole, which may cause problems when extrapolating to higher temperatures.

If CO data are not available, the models including PM_{10} and T have reasonable goodness-of-fit (r^2 = 0.67 for EF_{ufp} and 0.72 for $EF_{10–40}$), and other estimates can easily be derived from Tables 2 and 3.

Discussion

This study provides an easy and versatile method to estimate parameterisations for particle-number emission factors in terms of ambient conditions using data collected at a monitoring site. Generally, as pointed out previously[23] the emission factors derived with this method are comparable to those of previous International studies [13, 22, 31] and to our recent study of individual vehicles in the streets of Gothenburg within the same time frame.[32] The focus of the present study was on the influence of ambient conditions. Several different ways to estimate the EF from ambient variables were found, with the recommended

model being based on temperature and CO concentration. These two variables explained a high degree of the variation in the EF. In addition to the well-known effect of temperature on particle formation in the initial cooling and dilution of the exhaust, CO concentration acts as a proxy for the availability of condensation sinks. Regarding the effect of ambient temperature, one may compare our findings to previous field observations. Measurements from a study comparable to ours were presented by Kristensson et al.[33] and modelled by Olivares et al.[34] Figure 6 shows those data together with our data and suggested model estimates. The effect of temperature is similar, giving higher EFs for lower ambient temperatures in all three studies. However, our absolute EF is significant lower than that of the previous studies. Three main causes can be postulated: (1) differences in size-range applied, (2) different numbers of heavy duty vehicles, and (3) effects of aerosol transformations such as evaporation. The size range was only slightly larger, the number of heavy duty only slightly smaller, the change in sulphur content very limited, as Sweden reduced the sulphur in fuel several years before these studies. Still, this study shows rooftop emission factors compared to the street canyon emission factors of the other two studies[32,33].

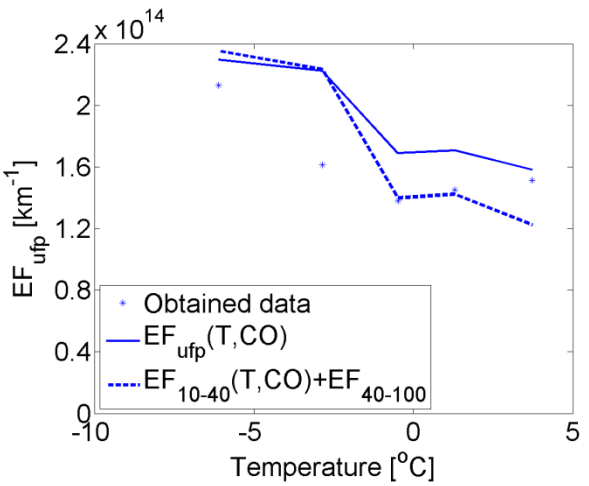

Fig. 5 EF_{ufp} versus temperature, obtained directly from the data (points), calculated from the regression analysis for EF_{ufp} according to Eq. 2 (solid line), and calculated as the sum of $EF_{10–40}$ and $EF_{40–100}$ from the regression analyses according to Eqs. 3 and 6 (broken line).

A study by Yao et al.[35] found a similar dependence of particle emissions on temperature and RH as in the present study. They sampled on-road and during higher ambient temperatures, which would give a similar total effect. Their temperature dependences were also stronger for smaller particle sizes. Jamriska et al.[36] found similar trends for the relationship between particle number and temperature, but much weaker correlations.

Their study was conducted during a summer season with substantially higher temperatures. Generally, negative temperature dependence has been attributed to the nucleation mode and to the nucleation of sulphuric acid.[37, 38] Charron and Harrison[39] found an emission factor increase of up to a factor of 10 for a ten degree temperature change. Our study did not see such a dramatic influence of temperature on EF, even if we did observe some effect, in contrast to a few other recent studies.[40, 41] One may note that the temperature interval in this study was limited, and rather cold compared to many places, meaning that one has to be careful when extrapolating the results to other environments. For very warm conditions, outside of the measured temperature range of this study, the predicted emissions become unrealistically low. In addition, the level of air pollution in the Gothenburg area is generally low to moderate, from an international perspective, in the absence of temperature inversions.[25]

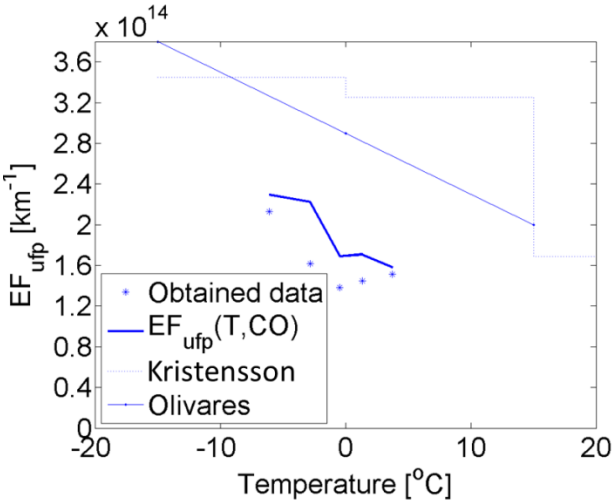

Fig. 6 EF_{ufp} versus temperature from the present study (data and regression estimate) compared with data from Kristensson et al. (2004) and the model of Olivares et al. (2007).

There are now a few studies showing diurnal variation in EFs, of up to 50%, that can be attributed to varying ambient conditions such as temperature or air quality.[18, 42] Virtanen et al.[43] found, in a study in Finland, that the number of particles from traffic was larger during the warm season, while Sabaliauskas et al.[44] found correlation between 8-50 nm sized particle concentrations and temperature, while no correlation was found between temperature and particles of larger sizes.

In our recommended model we used CO concentration as a proxy for available condensation sink. There have been no other studies to our knowledge using CO concentration to estimate particle-number emission factors. In the current study we also used PM_{10} concentration as a proxy. However, in urban areas PM_{10} may not fully capture the variability in surface area and one might expect, for example, $PM_{2.5}$ to be a better proxy. Alternatively, the surface area could be measured, for instance with an aerosol mass spectrometer (AMS), or the SMPS system could be set to run for a larger size interval, say 10–1000 nm. Unfortunately, such measurements are scarce for most monitoring sites in Europe, as air quality legislation regarding particles is currently based on PM_{10}, while emission standards are moving towards number-based limits.[31]

Conclusions

This study has shown the large variation in particle-number emission factors (EFs) for variable ambient conditions. The effect

is easily modelled using the presented methods, and equations to calculate EFs from readily available ambient data have been given. The effect of ambient conditions was found to be larger for the lower size-range of 10–40-nm particles than for 40–100-nm particles.

The method of Janhäll and Hallquist[23] for the estimation of size-segregated particle-number EFs, used in this study, has proven to be a valuable tool in describing the effect of different variables on the EFs.

The obtained equations have been used to describe the effects of temperature and air quality on EFs for the size-ranges 10–40 nm and 40–100 nm. Efforts were made to describe the air quality with the monitored air quality data, and CO concentration was chosen as the best available variable.

This study should be repeated for some of the nowadays frequently available datasets for traffic-affected areas that measure both the concentrations of CO, NO, and NO_2 and particle-size distributions, and have a larger variation in the tested parameters, which would reduce the statistical uncertainty. It would also be of great interest to use the model with data measured at different distances from the source.

This study recommends the use of the equation for traffic-related particle emissions in terms of CO and T, based on an EF_{NOx} of 1 g km^{-1}:

$$EF_{ufp} = 1.8\times10^{15}\times(1 - 0.095\times CO - 3.2\times10^{-3}\times T) \text{ particles km}^{-1}$$

One may also express the emission factors in two different size bins as below.

$$EF_{10-40} = 2.1\times10^{15}\times(1 - 0.099\times CO - 3.4\times10^{-3}\times T) \text{ particles km}^{-1}$$
$$EF_{40-100} = 3.9\times10^{13} \pm 1.1\times10^{13} \text{ particles km}^{-1}$$

These EFs describes the emissions from traffic as experienced at rooftop, or non–street canyon sites, i.e. after the dynamic tailpipe-to-road process.

Acknowledgements

MISTRA is acknowledged for funding. The authors are grateful to Miljöförvaltningen in Göteborg for providing data. This study was undertaken as part of the Göte-2005 measurement campaign.

Notes and references

[a] *VTI, the Swedish National Road and Transport Research Institute, Box 8072, SE-402 78 Göteborg, Sweden. Fax: +46 13 14 14 36; Tel: +46 31 7272608; E-mail: sara.janhall@vti.se*

[b] *Occupational and Environmental Medicine, University of Gothenburg, SE-405 30 Göteborg, Sweden. Tel: +46 31 7862857; E-mail: peter.molnar@amm.gu.se*

[c] *Atmospheric Science, Chemistry Department, University of Gothenburg, SE-412 96 Göteborg, Sweden; Tel: +46 31 7869019; E-mail: hallq@chem.se*

1. D. U. Keogh, J. Kelly, K. Mengersen, R. Jayaratne, L. Ferreira and L. Morawska, *Environmental Science and Pollution Research*, 2010, **17**, 724-739.
2. T. J. Grahame and R. B. Schlesinger, *Air Quality, Atmosphere and Health*, 2009, 1-25.
3. T. F. Mar, K. Ito, J. Q. Koenig, T. V. Larson, D. J. Eatough, R. C. Henry, E. Kim, F. Laden, R. Lall, L. Neas, M. Stolzel, P. Paatero, P. K. Hopke and G. D. Thurston, *Journal of Exposure Science and Environmental Epidemiology*, 2006, **16**, 311-320.
4. N. L. Mills, K. Donaldson, P. W. Hadoke, N. A. Boon, W. MacNee, F. R. Cassee, T. Sandstrom, A. Blomberg and D. E. Newby, *Nat Clin Pract Cardiovasc Med*, 2009, **6**, 36-44.
5. W. H. Roemer and J. H. van Wijnen, *Epidemiology*, 2001, **12**, 649-653.
6. G. Hoek, B. Brunekreef, S. Goldbohm, P. Fischer and P. A. van den Brandt, *Lancet*, 2002, **360**, 1203-1209.
7. M. Jerrett, R. T. Burnett, R. J. Ma, C. A. Pope, D. Krewski, K. B. Newbold, G. Thurston, Y. L. Shi, N. Finkelstein, E. E. Calle and M. J. Thun, *Epidemiology*, 2005, **16**, 727-736.
8. C. A. Pope and D. W. Dockery, *Journal of the Air & Waste Management Association*, 2006, **56**, 709-742.
9. R. B. Schlesinger, N. Kunzli, G. M. Hidy, T. Gotschi and M. Jerrett, *Inhal Toxicol*, 2006, **18**, 95-125.
10. P. C. Albuquerque, J. F. Gomes and J. C. Bordado, *Journal of the Air & Waste Management Association*, 2012, **62**, 373-380.
11. S. Hasegawa, M. Hirabayashi, S. Kobayashi, Y. Moriguchi, Y. Kondo, K. Tanabe and S. Wakamatsu, *Journal of Environmental Science and Health Part a-Toxic/Hazardous Substances & Environmental Engineering*, 2004, **39**, 2671-2690.
12. S. Janhall, A. M. Jonsson, P. Molnar, E. A. Svensson and M. Hallquist, *Atmospheric Environment*, 2004, **38**, 4331-4340.
13. L. Morawska, Z. Ristovski, E. R. Jayaratne, D. U. Keogh and X. Ling, *Atmospheric Environment*, 2008, **42**, 8113-8138.
14. T. Ronkko, A. Virtanen, K. Vaaraslahti, J. Keskinen, L. Pirjola and M. Lappi, *Atmospheric Environment*, 2006, **40**, 2893-2901.
15. K. M. Zhang and A. S. Wexler, *Atmospheric Environment*, 2002, **36**, 1863-1874.
16. M. Hallquist, J. C. Wenger, U. Baltensperger, Y. Rudich, D. Simpson, M. Claeys, J. Dommen, N. M. Donahue, C. George, A. H. Goldstein, J. F. Hamilton, H. Herrmann, T. Hoffmann, Y. Iinuma, M. Jang, M. E. Jenkin, J. L. Jimenez, A. Kiendler-Scharr, W. Maenhaut, G. McFiggans, T. F. Mentel, A. Monod, A. S. H. Prevot, J. H. Seinfeld, J. D. Surratt, R. Szmigielski and J. Wildt, *Atmospheric Chemistry and Physics*, 2009, **9**, 5155-5236.
17. A. L. Robinson, N. M. Donahue, M. K. Shrivastava, E. A. Weitkamp, A. M. Sage, A. P. Grieshop, T. E. Lane, J. R. Pierce and S. N. Pandis, *Science*, 2007, **315**, 1259-1262.
18. A. J. Kalafut-Pettibone, J. Wang, W. E. Eichinger, A. Clarke, S. A. Vay, D. R. Blake and C. O. Stanier, *Atmospheric Chemistry and Physics*, 2011, **11**, 8861-8881.
19. D. U. Keogh, L. Ferreira and L. Morawska, *Environmental Modelling & Software*, 2009, **24**, 1323-1331.
20. S. Janhall, M. O. Andreae and U. Poschl, *Atmospheric Chemistry and Physics*, 2010, **10**, 1427-1439.
21. P. Kumar, A. Garmory, M. Ketzel, R. Berkowicz and R. Britter, *Atmospheric Environment*, 2009, **43**, 949-958.
22. P. Kumar, B. R. Gurjar, A. S. Nagpure and R. M. Harrison, *Environmental Science & Technology*, 2011, **45**, 5514-5521.
23. S. Janhall and M. Hallquist, *Environmental Science & Technology*, 2005, **39**, 7609-7615.
24. J. Boman, M. J. Gatari, S. Janhäll, A. S. Shannigrahi and A. Wagner, *Atmospheric Chemistry and Physics*, 2009, **9**, 2607-2618.

25. S. Janhall, K. F. G. Olofson, P. U. Andersson, J. B. C. Pettersson and M. Hallquist, *Atmospheric Environment*, 2006, **40**, 5355-5366.
26. K. F. G. Olofson, P. U. Andersson, M. Hallquist, E. Ljungstrom, L. Tang, D. L. Chen and J. B. C. Pettersson, *Atmospheric Environment*, 2009, **43**, 340-346.
27. M. Svane, S. Janhall, M. Hagstrom, M. Hallquist and J. B. C. Pettersson, *Atmospheric Environment*, 2005, **39**, 6919-6930.
28. S. Szidat, M. Ruff, N. Perron, L. Wacker, H. A. Synal, M. Hallquist, A. S. Shannigrahi, K. E. Yttri, C. Dye and D. Simpson, *Atmospheric Chemistry and Physics*, 2009, **9**, 1521-1535.
29. J. Klingberg, L. Tang, D. Chen, G. Pihl Karlsson, E. Bäck and H. Pleijel, *Atmospheric Chemistry and Physics Discussion*, 2009, **9**, 2081-2111.
30. M. Paramonov, T. Gronholm and A. Virkkula, *Boreal Environment Research*, 2011, **16**, 304-320.
31. P. Kumar, M. Ketzel, S. Vardoulakis, L. Pirjola and R. Britter, *Journal of Aerosol Science*, 2011, **42**, 580-603.
32. C. S. Hak, M. Hallquist, E. Ljungstrom, M. Svane and J. B. C. Pettersson, *Atmospheric Environment*, 2009, **43**, 2481-2488.
33. A. Kristensson, C. Johansson, R. Westerholm, E. Swietlicki, L. Gidhagen, U. Wideqvist and V. Vesely, *Atmospheric Environment*, 2004, **38**, 657-673.
34. G. Olivares, C. Johansson, J. Strom and H. C. Hansson, *Atmospheric Environment*, 2007, **41**, 2145-2155.
35. X. Yao, N. T. Lau, C. K. Chan and M. Fang, *Atmospheric Environment*, 2007, **41**, 3328-3338.
36. M. Jamriska, L. Morawska and K. Mergersen, *Atmospheric Environment*, 2008, **42**, 2369-2382.
37. M. Lemmetty, L. Pirjola, J. M. Makela, T. Ronkko and J. Keskinen, *Journal of Aerosol Science*, 2006, **37**, 1596-1604.
38. J. P. Shi and R. M. Harrison, *Environmental Science & Technology*, 1999, **33**, 3730-3736.
39. A. Charron and R. M. Harrison, *Atmospheric Environment*, 2003, **37**, 4109-4119.
40. R. Casati, V. Scheer, R. Vogt and T. Benter, *Atmospheric Environment*, 2007, **41**, 2125-2135.
41. B. Wehner, U. Uhrner, S. von Lowis, M. Zallinger and A. Wiedensohler, *Atmospheric Environment*, 2009, **43**, 1235-1245.
42. W. Birmili, B. Alaviippola, D. Hinneburg, O. Knoth, T. Tuch, J. Borken-Kleefeld and A. Schacht, *Atmospheric Chemistry and Physics*, 2009, **9**, 2355-2374.
43. A. Virtanen, T. Ronkko, J. Kannosto, J. Ristimaki, J. M. Makela, J. Keskinen, T. Pakkanen, R. Hillamo, L. Pirjola and K. Hameri, *Atmospheric Chemistry and Physics*, 2006, **6**, 2411-2421.
44. K. Sabaliauskas, C.-H. Jeong, X. Yao, Y.-S. Jun, P. Jadidian and G. J. Evans, *Atmospheric Environment*, 2012, **49**, 245-256.